Title	The Impact of Surfactant Sodium Dodecyl Sulfate on the Microstructure and Thermoelectric Properties of p-type (Sb1-xBix)2Te3 Electrodeposited Films
Authors	Lal, Swatchith;Gautam, Devendraprakash;Razeeb, Kafil M.
Publication date	2016-12-22
Original Citation	Lal, S., Gautam, D. and Razeeb, K. M. (2017) 'The Impact of Surfactant Sodium Dodecyl Sulfate on the Microstructure and Thermoelectric Properties of p-type (Sb1-xBix)2Te3 Electrodeposited Films', ECS Journal of Solid State Science and Technology, 6(3), pp. N3017-N3021. doi:10.1149/2.0041703jss
Type of publication	Article (peer-reviewed)
Link to publisher's version	10.1149/2.0041703jss
Rights	
Download date	2024-04-19 00:19:05
Item downloaded from	https://hdl.handle.net/10468/3526

The Impact of Surfactant Sodium Dodecyl Sulfate on the Microstructure and Thermoelectric Properties of p-type (Sb$_{1-x}$Bi$_x$)$_2$Te$_3$ Electrodeposited Films

Swatchith Lal, Devendraprakash Gautam, and Kafil M. Razeeb[*,z]

Tyndall National Institute, University College Cork, Lee Maltings, Cork T12 R5CP, Ireland

This work reports on the synthesis of p-type (Sb$_{1-x}$Bi$_x$)$_2$Te$_3$ thin films using pulsed electrodeposition with and without the presence of an anionic surfactant, sodium dodecyl sulfate (SDS). The effect of SDS on the morphology of the films was investigated, and it was found that films with SDS in the electrolyte were smooth and denser as compared to the films without SDS. Post-deposition annealing of the films resulted in preferential crystal orientation. The Seebeck coefficient showed an improvement of 49% for the films deposited with SDS, which improved the overall power factor of the films by 143%.

Data traffic is projected to increase sharply (40-80× by 2020) and this is driving an increase in network complexity and the requirement for scalable optoelectronic integration.[1] A major bottleneck to this large scale integration is thermal management. Active photonic devices generate extremely high heat flux levels ($\sim$10 kW/cm^2) that must be efficiently removed to maintain performance and reliability; furthermore, active photonic devices must be controlled at temperature precision better than ±0.1°C. Today's thermal technology is at the limit and cannot scale with growth in the network.[2]

Current state-of-the-art thermal design of Photonic Integrated Circuits (PICs) is unable to meet the challenge in data traffic over the coming years. Today's PICs employ macro thermoelectric cooler (TEC) that are inefficient in thermal management of the device. Micro-TEC integrated directly on the laser can more efficiently manage thermal cooling of the device. The aim of TIPS project[2] is to develop novel p and n type thermoelectric materials, and to design and develop a micro-thermoelectric cooler (μ-TEC), integrated around the PIC, which can effectively remove heat from the photonic system. As a part of this work, we have been trying to enhance the structural and thermoelectric (TE) properties of bismuth telluride based materials. Binary semiconductor Bismuth Telluride Bi-Te based materials have been extensively studied, and applied in thermoelectric generators (TEG) and thermoelectric coolers (TEC) devices because of their unique properties, which exhibit better figure of merit (ZT) near room temperature regime.[3–6]

The efficiency of the thermoelectric films are evaluated in terms of dimensionless figure of merit *ZT*, which can be expressed as,

$$ZT = \frac{S^2\sigma}{\kappa}T$$

where *S*, σ, *T* and *k* are the Seebeck coefficient, the electrical conductivity, the absolute temperature and the thermal conductivity respectively. Therefore, for superior thermoelectric properties, *ZT* should be high, for which the Seebeck coefficient and the electrical conductivity must be high and the thermal conductivity should be low.[7,8] Two strategies are generally used to enhance the thermoelectric efficiency of the materials, (1) to minimize the thermal conductivity and/or (2) to enhance the power factor (PF). In the present work we focused on improving the PF of the materials, where PF = $S^2\sigma$.

The electrochemical deposition is extensively used for the synthesis of the device fabrication due to suitability of the technique for its cost effectiveness, up-scalability and ease of controlling film properties such as composition, crystallinity and morphology.[9,10]

In the fabrication of micro-thermoelectric devices, one of the challenges to overcome is to reduce the roughness of the films. The electrodeposited BiTe based materials are dendritic and rough.[11,12] Thereby, the focus of the present work is to reduce the morphological defects and produce smoother films, without sacrificing the Seebeck coefficient. Here, we studied the addition of a surfactant that modifies the interfacial tension between the solution and the electrode which enables the ease of escape to the gas bubbles from the electrode surface, due to which the formation of pinholes and pitting can be eliminated.[13] Researchers have been working to improve these properties by the addition of surfactant. In order to make the films homogeneous and smooth, different surfactants have been used namely sodium ligninsulfonate (SLS),[14,15] cetyltrimethylammonium bromide CTAB,[16,17] ethylene-glycol,[18] polyvinylpyrrolidone (PVP), and sodium dodecyl sulfate (SDS).[19] However, most of the reported works are done on n-type Bi$_2$Te$_3$. There has been only one paper in the literature that reported on improving the homogeneity of electroplated p-type Bi$_{0.5}$Sb$_{1.5}$Te$_3$ by using surfactants.[20] It was shown that the addition of sodium ligninsulfonate improved the homogeneity of the films without changing the crystallographic orientation of the films and also improved the Seebeck coefficient as compared to films without any surfactant. Thereby, in the present work we demonstrate smooth and dense films of p-type bismuth antimony telluride (Bi-Sb-Te) synthesized by pulsed electrodeposited using SDS as a surfactant. Pulsed plating is an advanced form of electrodeposition compared to the conventional potentiostatic or galvanostatic deposition. It has several advantages such as synthesis of uniform films with fine grains and low porosity, better and crack free adhesion and reduction in the surface roughness.[11] Furthermore, we investigated and compared morphology, crystallinity, composition and the thermoelectric properties of the electrodeposited films with and without SDS after annealing for 1 h at 350°C in N$_2$ atmosphere.

Experimental

Bismuth (III) nitrate pentahydrate (ACS reagent ≥98.0%), antimony (III) oxide, tellurium (powder 200mesh, 99.8% trace metals basis), sodium dodecyl sulfate (SDS) (BioReagent ≥99.5%), tartaric acid (ACS reagent ≥99.5%), nitric acid (ACS reagent ≥69%) and

*Electrochemical Society Member.
zE-mail: kafil.mahmood@tyndall.ie

dimethyl sulfoxide (ACS reagent $\geq 99.9\%$) were used for the experiments as received.

In preparing solution (A), 15 mM of tellurium (Te) was put into 25 mL of 1 M HNO_3 and was heated at $45°C$ to dissolve Te completely and 5 mM $Bi(NO_3)_3 \cdot 5H_2O$ was added to the solution. Solution (B) was prepared using 5 mM Sb_2O_3 in 25 mL of 0.2 M tartaric acid and was heated at $45°C$ for proper dissolution. Two solutions A and B were mixed and 50 mL of dimethyl sulfoxide (DMSO) was added to the mixed solutions. The whole solution was maintained at 1:1 ratio of DI water and DMSO. SDS was added at different concentrations ranging from 0.2 mM to 2.0 mM in the solution while stirring.

Experiments were carried out in a three-electrode setup at room temperature. The electrodeposition potential was controlled by CHI600 series electrochemical analyzer/workstation. The reference electrode was Ag/AgCl. A platinized titanium mesh was used as the counter electrode. In order to determine the reduction potentials, cyclic voltammetry (CV) was performed between the fixed potentials of -0.6 V and 0.8 V vs Ag/AgCl at a scan rate of 10 mV/s. Films were deposited by triple pulse amperometry technique on a square (32 mm $\times$ 32 mm) Si/SiO_2 substrate, having 20 nm Au layer on the top of 10 nm Ti layer. No magnetic stirring was used and all the depositions were performed at ambient room temperature of $25°C$. The substrates were cleaned with ethanol and then with deionized (DI) water in an ultrasonic bath and finally dried by blowing nitrogen at ambient temperature before deposition. The films deposited with and without SDS were annealed at $350°C$ for 1 h in N_2 atmosphere at a ramp rate of 5 K/min in order to enhance their thermoelectric properties.

X-ray diffraction patterns (XRD) were measured by X-Ray diffractometer Pan analytical X'pert pro, using Cu K_α radiation at a voltage of 40 kV and a current of 40 mA. The morphology and elemental composition of the obtained films were analyzed using a scanning electron microscope (SEM) Quanta FEG 450 at an accelerating voltage of 15 kV, coupled with an energy dispersive spectrometer (EDS).

Electrical properties were measured using a four point probe measurement system (Jandel RM300). Laboratory built Seebeck-measurement system was used to measure the Seebeck coefficient of the electrodeposited films. The temperature gradient (ΔT) was established along the ends of the film using commercially available thermoelectric coolers. The thermovoltage produced due to the temperature difference was measured using a high impedance electrometer. Temperatures of the hot and cold ends were measured using two separate thermocouples. The samples were measured for Seebeck coefficient at different ΔT values from 2–10°C. Necessary calibrations were done to ensure the accuracy of the system.

Results and Discussion

In order to determine the appropriate reduction potential range and to investigate the underlying electrochemical reaction, cyclic voltammograms (CVs) were recorded, using gold as a working electrode immersed in an electrolyte containing Bi^{+3}, SbO^+ and $HTeO_2^+$ ions with and without the presence of SDS in the electrolyte. Figure 1a shows the voltammograms of the solutions with and without SDS measured on the standard gold electrode of 1 mm radius with a scan rate of 10 mV/s. Both the CVs reveal three cathodic peaks at potentials of -0.07, -0.15 and -0.27 V vs. Ag/AgCl, which may be attributed to the reduction of Bi, Te and Sb, respectively.[20] Different concentrations of SDS ranging from 0.2 to 2 mM were analyzed and no significant change was observed in the CVs as can be seen in Figure S1 of the supplementary information (SI) section and illustrated for 0.8 mM SDS in Figure 1a. Based on these studies, the reduction potentials were fixed for the deposition of the films using triple pulse amperometry technique as shown in Figure 1b, where the chosen pulse potentials were V1 = -80 mV for a duration of 10 ms, V2 = -50 mV for a duration 50 ms and V3 = -300 mV for a duration of 10 ms. The total duration of deposition of the films was fixed to 3600 s and the film thickness obtained was approximately 2.0 μm with this deposition time.
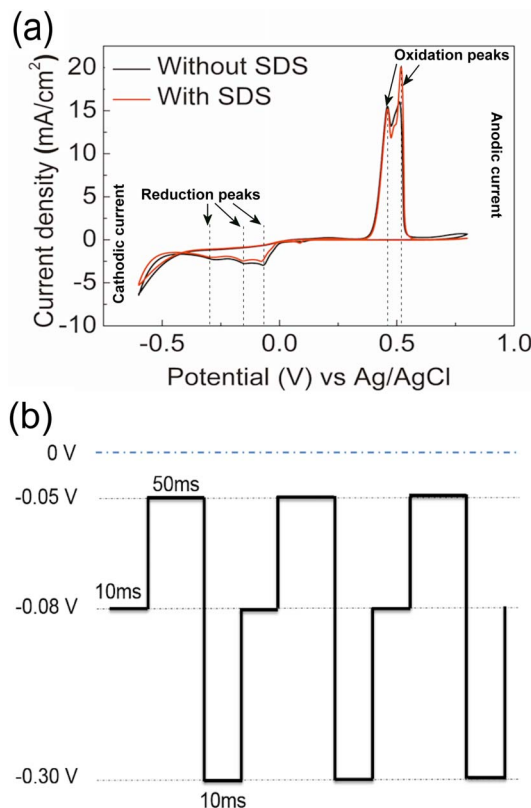

Figure 1. (a) Cyclic voltammograms of gold working electrode without and with 0.8 mM SDS. All the voltammograms were recorded at room temperature at a scan rate of 10 mVs^{-1} (b) Schematic of triple pulse deposition potentials.

As a preliminary characterization, in order to observe the morphological change, SEM images were taken of the films without and with various concentration of SDS. It was observed that from 0.8 mM concentration of SDS, films started to change from fibrous to granular morphology and thereby further studies were focused on 0.8 mM SDS samples where 0.4 mM SDS films were also used for a better understanding.

The SEM image in Figure 2a shows the surface morphology of the electrodeposited Bi-Sb-Te thin films without SDS. The film shows a fibrous dendritic structure, which is rough and porous. For the 0.4 mM SDS film (Figure 2b), no major change in the morphology is observed. However, the SEM of 0.8 mM film in Figure 2c shows a granular structure, which reveals that in the presence of 0.8 mM SDS the morphology changed drastically and the films became denser. The density of the films was calculated from the weight of the deposit and total volume of the film. It was found that the films with 0.8 mM SDS have an average density of 6.11 g/cm^3 as compared to 5.64 g/cm^3 for the films without SDS. The cross-sectional images of the films are shown in Figure 3, where Figure 3a shows the film without SDS, which is rough and indicates rough deposition with a high porosity. Whereas, the film with 0.8 mM SDS shows significant improvement in terms of uniformity and smooth profile as can be seen in Figure 3b.

The composition of the films was determined by EDX analysis. Table I shows the atomic percentages of different constituents and a comparison between the films without and with surfactant of different concentrations. Due to the addition of SDS in the electrolyte, bismuth and tellurium contents in the films increased and antimony content decreased. Both of the films with and without SDS were annealed at $350°C$ for 1 h. It was observed that the tellurium content starts depleting when annealed at $350°C$ for both films, which may be due to the evaporation of tellurium at high temperatures. Table II exhibits the analyzed composition of the films before and after annealing with different concentrations of SDS.
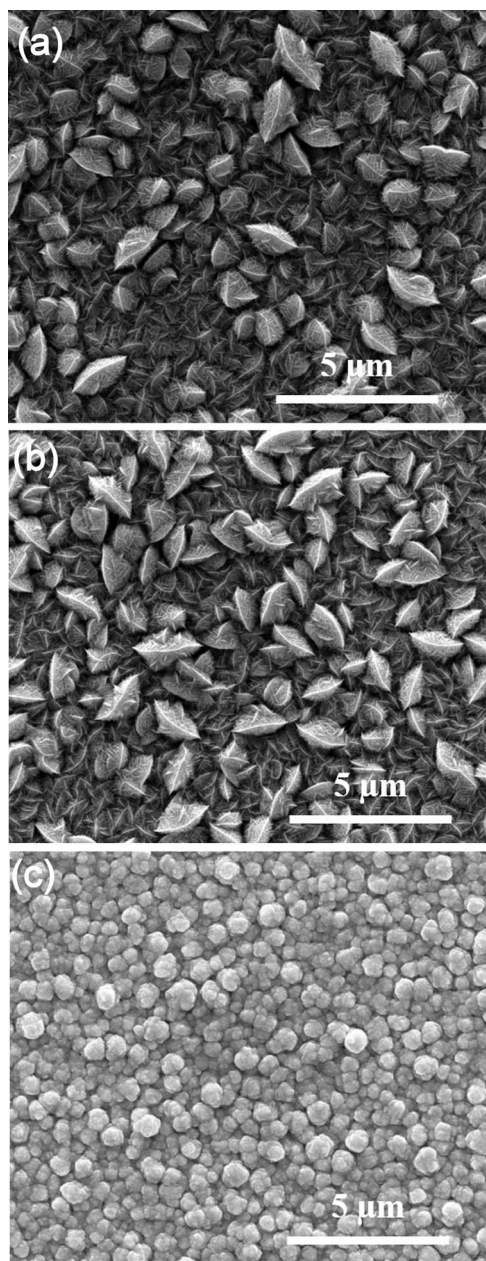
Figure 3. Cross-sectional images of with and without SDS (a) without SDS (b) with 0.8 mM SDS.

peak becomes more intense. XRD studies reveal that the SDS impacts the growth of (110) peak and it gradually wanes and diminishes for films of the case of 0.8 mM SDS (see Figure 4a). On annealing the films become more crystalline with (015) peak still stays as a prominent peak. (110) peak is observed in 0.8 mM SDS sample after annealing along with some more peaks as shown in Figure 4b. $AuTe_2$ peak was observed after annealing, which may be due to the reaction of Au from the seed layer with tellurium from the film at elevated temperatures to form $AuTe_2$. The average crystallite size of the as-deposited films was measured from the XRD data using the Debye-Scherrer formula, and is shown in Table III. It was observed that the average crystallite size increases with the addition of SDS from 13.5 nm to 17.6 nm. This observation relates that the SDS concentration has a direct impact on the crystallite size. On annealing, it further increases where the average crystallite size of the annealed films without SDS was 27.7 nm and 31.6 nm for the films with 0.8 mM SDS. One of the probable reasons for the change in the microstructure of the films from rough to granular structure (see Figures 2 and 3) could result from the anisotropy in adsorption stability of SDS molecules in the electrolyte. The SDS molecule tends to adsorb along (110) plane

Figure 2. (a) SEM images of as-deposited samples (a) without SDS (b) 0.4 mM SDS and (c) 0.8 mM SDS.

Figure 4a shows the XRD patterns of the films electrodeposited without SDS and with 0.4 and 0.8 mM SDS. All the films have a rhombohedral crystal structure of $(Sb_{1-X} Bi_X)_2Te_3$ (ICSD PDF card (72-1835)). The (015) was the preferred orientation detected at $2\theta \sim 27.6$ for all the films. From the XRD, it can be observed that the (110) peak present in films without SDS and 0.4 mM SDS while it is absent in 0.8 mM SDS films. With 0.8 mM SDS concentration, (015)
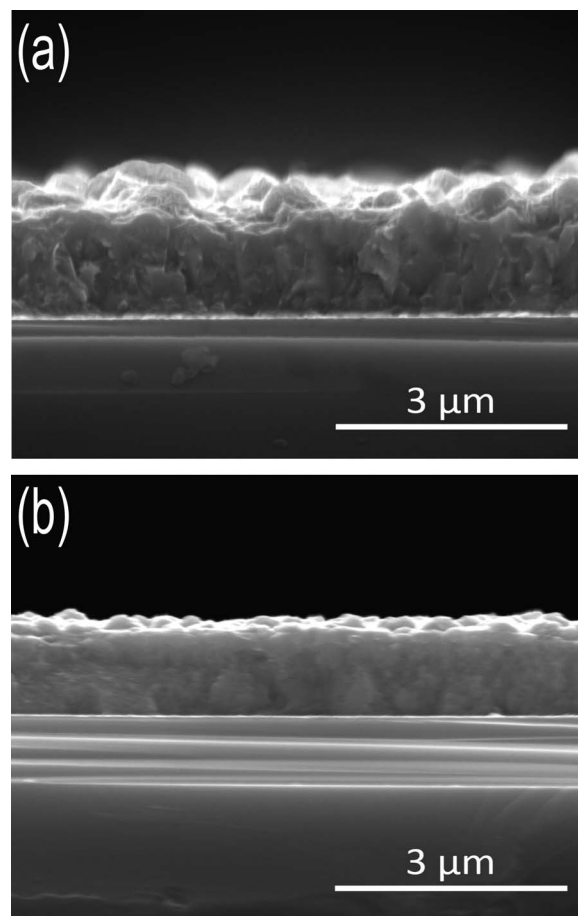
Table I. Atomic composition of Bi-Sb-Te films with different concentrations of SDS in electrolyte and change in the composition after annealing.

Concentration of SDS (mM)	Film composition (%)			Film composition (%) Annealed at 350°C		
	Sb	Te	Bi	Sb	Te	Bi
0	20.49	61.34	18.18	21.78	59.81	18.42
0.4	18.99	62.23	18.78	20.47	60.09	19.45
0.8	13.59	64.92	21.50	15.28	61.80	22.93

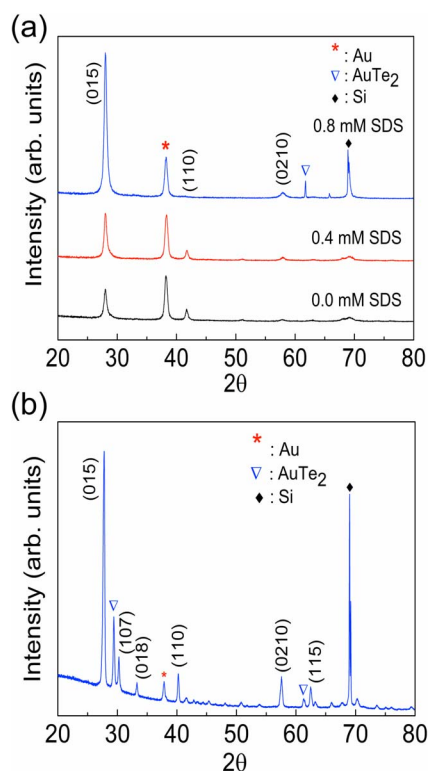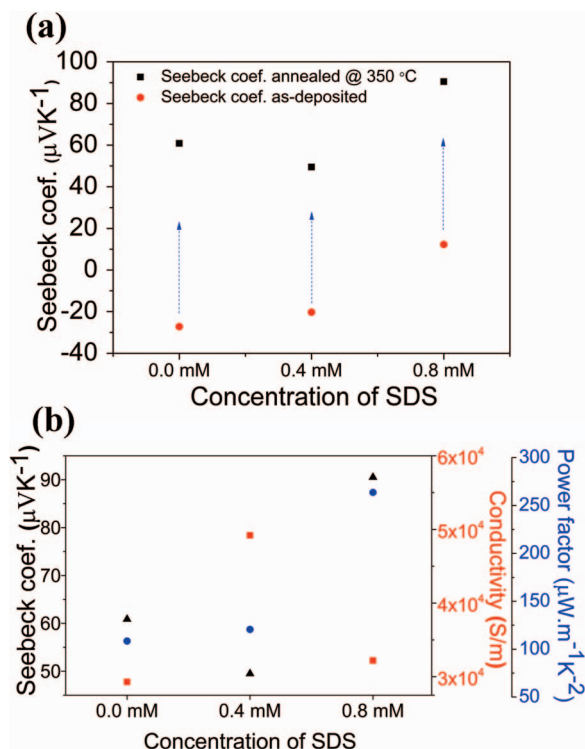**Table II. Composition of Bi-Sb-Te films with different concentrations of SDS before and after annealing.**

Concentration of SDS (mM)	As-deposited	Annealed at 350°C
0.0	$(Sb_{1.02}Bi_{0.91})_2Te_{3.07}$	$(Sb_{1.09}Bi_{0.92})_2Te_{3.00}$
0.4	$(Sb_{0.95}Bi_{0.94})_2Te_{3.11}$	$(Sb_{1.02}Bi_{0.97})_2Te_{3.00}$
0.8	$(Sb_{0.68}Bi_{1.10})_2Te_{3.25}$	$(Sb_{0.76}Bi_{1.15})_2Te_{3.09}$

Table III. Average crystallite size of films prepared with different concentrations of SDS.

Samples	Crystallite size (nm) As-deposited	Crystallite size (nm) After annealing
0.0 mM SDS	13.5	27.7
0.4 mM SDS	14.5	27.1
0.8 mM SDS	17.6	31.6

thereby lowering its surface energy and hindering growth along this direction in agreement with the XRD data shown in Figure 4a, where (110) peak intensity gradually decreases with increasing SDS concentration. The decrease in the surface projections and surface energy leads to smoother microstructure. Similar observation was seen on electrodeposited $CuInSe_2$ on Mo substrate.[21]

Figure 5a shows the Seebeck coefficient of the samples deposited with and without SDS before and after annealing. The Seebeck coefficient of the as-deposited sample without SDS was $-27.22 \, \mu V/K$, which on annealing increased to $60.85 \, \mu V/K$ indicating not only the increment in the absolute value of the Seebeck coefficient but also the nature of the charge carriers change from *n*-type electron to *p*-type holes. However, for 0.8 mM SDS thin films the Seebeck coefficient of as-deposited samples showed a value of $12.22 \, \mu V/K$, which on annealing increased to $90.5 \, \mu V/K$ that is almost 49% higher than the values obtained from the films without SDS. The thermoelectric properties and electrical conductivities of the annealed Bi-Sb-Te thin films are shown in Figure 5b. There has been no drastic change observed in the electrical conductivities of films with different concentrations of SDS. The electrical conductivities of the films are in the order of 10^4 S/m with an optimum value of 5×10^4 S/m observed for 0.4 mM SDS. Annealing decreases the conductivity of the films compared to as-deposited films, and this may be due to decrease in the tellurium content in the films. Electrical conductivity measurements before and after annealing the films of different concentrations can be seen in Figure S3. Currently, there is no unambiguous understanding on the

Figure 5. (a) Seebeck measurement of as-deposited films with different concentrations of SDS and their comparison with values obtained post-annealing; (b) Electrical and thermoelectric properties of annealed films deposited with different concentrations of SDS.

enhancement of the Seebeck coefficient with SDS. One of the probable hypotheses[22,23] could be due to the role of Te in the film. As exhibited in Table I, the content of Te in as-deposited with SDS is reasonably high compared to without SDS samples. Annealing the film results in Te depletion, however, the absolute value of Te remains higher compared to films without SDS (see Table I). Thus, the Seebeck coefficient of films without SDS is lower than compared to 0.8 mM SDS. The power factor of the films without SDS was $108.48 \, \mu W.m^{-1}K^{-2}$, which on addition of 0.4 mM SDS raised to $120.55 \, \mu W.m^{-1}K^{-2}$ and with 0.8 mM SDS concentration in the electrolyte, films exhibited a power factor of $263.72 \, \mu W.m^{-1}K^{-2}$ which is 143% higher than the power factor of without SDS films. Further work is needed to investigate in detail the impact of SDS on the thermoelectric properties.

Conclusions

This study demonstrates that the surfactant SDS improved the quality and surface smoothness of p-type $(Sb_{1-X}Bi_X)_2Te_3$ films. SEM images reveal that the SDS contributes in reducing the surface roughness and the films obtained were compact, overcoming the porous nature of the films without SDS. XRD studies revealed the growth of the average crystallite size with the increasing concentration of SDS. Furthermore, the films deposited with surfactant showed a Seebeck coefficient value of $90.5 \, \mu V/K$ post annealing, which is 49% higher

Figure 4. (a) XRD of as-deposited films with different concentrations of SDS, (b) Annealed 0.8 mM SDS.

as compared to the film without surfactant. Due to which, a power factor of 263.72 μW/mK^2 was achieved, which is more than twice of the value for the films deposited without SDS.

References

1. J. Brodkin, *Arstechnica*, http://arstechnica.com/business/2012/2005/bandwidth-explosion-as-internet-use-soars-can-bottlenecks-be-averted/ (2014).
2. R. Enright, S. Lei, K. Nolan, I. Mathews, A. Shen, G. Levaufre, R. Frizzell, G. H. Duan, and D. Hernon, *Bell Labs. Tech. J.*, **19**, 31 (2014).
3. R. Rostek, N. Stein, and C. Boulanger, *J. Mater. Res.*, **30**(17), 2518 (2015).
4. R. Venkatasubramanian, E. Siivola, T. Colpitts, and B. O'Quinn, *Nature*, **413**(6856), 597 (2001).
5. F. J. Disalvo, *Science*, **285**(5428), 703 (1999).
6. L. E. Bell, *Science*, **321**(5895), 1457 (2008).
7. X. Zhang and L.-D. Zhao, *J. Materiomics.*, **1**(2), 92 (2015).
8. G. J. Snyder and E. S. Toberer, *Nat Mater*, **7**(2), 105 (2008).
9. C. Boulanger, *J. Electron. Mater.*, **39**(9), 1818 (2010).
10. F. Xiao, C. Hangarter, B. Yoo, Y. Rheem, K.-H. Lee, and N. V. Myung, *Electrochim. Acta.*, **53**(28), 8103 (2008).
11. D. D. Frari, S. Diliberto, N. Stein, C. Boulanger, and J.-M. Lecuire, *J. Appl. Electrochem.*, **36**(4), 449 (2006).
12. F. Li and W. Wang, *Appl. Surf. Sci.*, **255**(7), 4225 (2009).
13. R. Vittal, H. Gomathi, and K.-J. Kim, *Adv. Colloid. Interfac.*, **119**(1), 55 (2006).
14. O. Caballero-Calero, P. Díaz-Chao, B. Abad, C. V. Manzano, M. D. Ynsa, J. J. Romero, M. M. Rojo, and M. S. Martín-González, *Electrochim. Acta.*, **123**, 117 (2014).
15. A. J. Naylor, E. Koukharenko, I. S. Nandhakumar, and N. M. White, *Langmuir*, **28**(22), 8296 (2012).
16. Y. Song, I.-J. Yoo, N.-R. Heo, D. C. Lim, D. Lee, J. Y. Lee, K. H. Lee, K.-H. Kim, and J.-H. Lim, *Curr. Appl. Phys.*, **15**(3), 261 (2015).
17. I.-J. Yoo, Y. Song, D. Chan Lim, N. V. Myung, K. H. Lee, M. Oh, D. Lee, Y. D. Kim, S. Kim, Y.-H. Choa, J. Y. Lee, K. H. Lee, and J.-H. Lim, *J. Mater. Chem. A*, **1**(17), 5430 (2013).
18. M. Wu, H. P. Nguyen, R. J. M. Vullers, P. M. Vereecken, K. Binnemans, and J. Fransaer, *J. Electrochem. Soc.*, **160**(4), D196 (2013).
19. K. Chiranjit, M. Mousumi, K. Kajari, G. Saibal, B. Dipali, and G. Shyamaprosad, *Mater. Res. Express*, **2**(10), 106403 (2015).
20. J. Kuleshova, E. Koukharenko, X. Li, N. Frety, I. S. Nandhakumar, J. Tudor, S. P. Beeby, and N. M. White, *Langmuir*, **26**(22), 16980 (2010).
21. P.-K. Hung, H.-G. Cai, K.-C. Huang, and M.-P. Houng, *J. Electrochem. Soc.*, **160**(1), D1 (2013).
22. K. M. Razeeb and D. Gautam, Alloy System with Enhanced Seebeck Coefficient and Process for Making Same, U.S. Serial No. 62/240,197, (2015).
23. D. Gautam, E. Dalton, and K. M. Razeeb; "Innovative method to enhance Seebeck coefficient of annealed p-type $(Sb_{1-x}Bi_x)_2Te_3$", *Adv. Energy Mater.*, (to be communicated soon).